Hematological Oncology
Hematol Oncol 2015; **33**: 239–246
Published online 18 August 2014 in Wiley Online Library
(wileyonlinelibrary.com) **DOI**: 10.1002/hon.2158

Case Report

MLL/KMT2A translocations in diffuse large B-cell lymphomas

Tatyana Gindin, Vundavalli Murty, Bachir Alobeid and Govind Bhagat*

Department of Pathology and Cell Biology, Columbia University Medical Center and New York Presbyterian Hospital, New York, NY, 10032, USA

**Correspondence to: Govind Bhagat M.D., Department of Pathology and Cell Biology, Columbia University Medical Center, New York Presbyterian Hospital, VC14-228, 630W 168th street New York, NY 10032, USA. E-mail: gb96@cumc.columbia.edu*

Received 23 June 2014
Revised 8 July 2014
Accepted 9 July 2014

Abstract

Translocations of the histone-lysine *N*-methyltransferase 2A (*KMT2A*) gene, formerly known as myeloid lymphoid leukemia/mixed-lineage leukemia gene, are commonly associated with high-risk *de novo* or therapy-associated B-cell and T-cell lymphoblastic leukemias and myeloid neoplasms. Rare B-cell non-Hodgkin lymphomas harboring *KMT2A* translocations have been reported, but information regarding the clinical behavior of such cases is limited. Here, we describe two extranodal diffuse large B-cell lymphomas (DLBCLs): a primary thyroid DLBCL and a large cell transformation of a splenic marginal zone lymphoma, which displayed complex karyotypes and translocations involving chromosome 11q23 targeting the *KMT2A* gene. The pathological and clinical characteristics of these cases are discussed in the context of previously reported lymphomas associated with different types of *KMT2A* genetic aberrations. In contrast to the poor clinical outcomes of patients with acute leukemias and myeloid neoplasms associated with *KMT2A* translocations, patients with B-cell non-Hodgkin lymphomas, exhibiting similar translocations, appear to respond well to immunochemotherapy. Our findings add to the growing list of histone methyltransferase genes deregulated in DLBCL and highlight the diversity of mechanisms, altering the function of epigenetic modifier genes in lymphomas.

Keywords: diffuse large B-cell lymphoma; cytogenetics; *MLL*; *KMT2A*; translocation; rearrangement

Introduction

Diffuse large B-cell lymphomas (DLBCLs) are the most common type of non-Hodgkin lymphomas (NHLs), accounting for over 30% of all NHL. These neoplasms comprise a heterogeneous group with respect to morphologic, phenotypic, and genetic characteristics [1,2], which is reflected in their disparate clinical behaviour and response to therapy (overall 5-year survival range 10–60%) [3]. Despite extensive investigations into the genetic underpinnings of DLBCLs over the past couple of decades, the molecular mechanisms involved in disease initiation and progression are still not well understood. Most DLBCLs are characterized by complex karyotypes including multiple chromosomal gains, losses, and translocations [4,5].

Cytogenetic aberrations of the histone-lysine N-methyltransferase 2A (*KMT2A*) gene, previously also referred to as the myeloid lymphoid leukemia/mixed-lineage leukemia (*MLL*), trithorax-like protein, CXXC-type zinc finger protein 7 and zinc finger protein HRX gene, amongst others, have been extensively studied in B-cell and T-cell lymphoblastic leukemias, acute myeloid leukemias and myelodysplastic syndromes, where they have been implicated in disease pathogenesis [6]. Although chromosome 11q abnormalities are not infrequent in B-NHL [7], little is known about the presence or frequency of *KMT2A* aberrations and their prognostic impact in these neoplasms, primarily due to the rarity of well documented cases [8–11]. Here, we describe two unusual extranodal diffuse large B-cell lymphomas associated with *KMT2A* translocations, comprising a primary thyroid DLBCL and a large cell transformation of splenic marginal zone lymphoma (SMZL). These cases inform us of the broad range of neoplasms associated with *KMT2A* aberrations and suggest interrogation of the *KMT2A* gene by cytogenetic or genomic analysis when chromosome 11q23 abnormalities are encountered in B-NHL. Such analyses will reveal the spectrum of lymphomas associated with *KMT2A* aberrations and provide further insights into the role of *KMT2A* in mature B-cell neoplasia.

Case summaries

Case 1

A 70-year-old male with hypertension and long standing hypothyroidism presented to our institution due to a rapidly enlarging right neck mass causing hoarseness and upper airway obstruction, over a 6-month period. On physical examination, diffuse enlargement of the thyroid gland was noted, but no lymphadenopathy or organomegaly was evident. Computerized tomography scan of the neck demonstrated a mass arising in the thyroid and extending into

cervical soft tissue. An incisional biopsy was performed, which disclosed a DLBCL. The patient was treated with six cycles of R-CHOP chemotherapy (cyclophosphamide, hydroxydaunomycin, vincristine, prednisone and rituximab). Follow-up clinical evaluation and computerized tomography scans, 8 months post-chemotherapy, were consistent with complete remission, and the patient remains disease free 7 years after diagnosis.

Case 2

A 68-year-old female with a history of paroxysmal atrial fibrillation and progressive polyneuropathy, diagnosed as Guillain-Barre Syndrome, was initially treated with steroids, intravenous immune globulin and plasmapharesis, with good response. She presented to our institution with exacerbation of polyneuropathy requiring intubation. Given the atypical relapsing course of her disease, a search for an underlying neoplastic disorder was initiated. Bone marrow biopsy and peripheral blood flow cytometry were indicative of a low-grade B-NHL. Serum protein electrophoresis detected monoclonal IgM kappa paraprotein (1.4 g/dL). A positron emission tomography scan showed hypermetabolic lesions in the spleen and splenic hilar lymphadenopathy. A diagnosis of SMZL with transformation to DLBCL was rendered on evaluation of the splenectomy specimen. Chemotherapy with R-CHOP regimen was initiated. Repeat positron emission tomography scan and clinical evaluation after completion of six cycles of chemotherapy showed no evidence of disease. The patient remains in complete remission 2.5 years after diagnosis.

Methods

Formalin-fixed and paraffin-embedded tissue sections were stained with hematoxylin and eosin for morphologic evaluation. Immunohistochemical staining was performed with the following antibodies: CD3, CD5, CD20, CD43, BCL2, BCL6, CD10 (Leica Biosystems, Buffalo Grove, IL) and CD79a, Ki-67, MUM1 and p53 (Ventana Medical Systems, Oro Valley, AZ), after moist heat induced antigen retrieval. The Envision plus system (DAKO, Carpinteria, CA) and diaminobenzidine were used for visualization, according to standard methods. *In situ* hybridization for kappa and lambda light chain mRNA was performed according to standard methods (Ventana Medical Systems, Oro Valley, AZ). Four-colour flow cytometry of the fresh tissue samples was performed using a comprehensive panel of antibodies with FACSCalibur (Becton Dickinson, San Diego, CA). Data were analysed using Cellquest software (Becton Dickinson). G-banding was performed on metaphases obtained after overnight (12–15 h), unstimulated cultures, using standard procedures and karyotypes, were described according to the International System for Human Cytogenetic Nomenclature (ISCN 2009) [12]. Fluorescence *in situ* hybridization (FISH) analysis was performed on methanol–acetic acid fixed cells using dual-colour break-apart probes for *MLL/KMT2A*, *IGH*, *BCL2* and *BCL6*, as well as *ATM/TP53* locus-specific probes (VYSIS, Downers Grove, IL) according to standard protocols. Fluorescence signals were captured after counterstaining with DAPI using the Cytovision Imaging system attached to a Nikon Eclipse 600 microscope (Applied Imaging, Santa Clara, CA) and hybridization signals were scored in 200–500 cells. Polymerase chain reaction (PCR) analysis was performed to detect immunoglobulin heavy chain (*IGH*) gene rearrangement using DNA extracted from formalin-fixed, paraffin-embedded tissues [13].

This study was performed in accordance with the regulations of the Columbia University Human Research Protection Program, adhering to the ethical standards promulgated in the Helsinki Declaration, and a protocol approved by the Institutional Review Board of Columbia University, New York, USA.

Results

Case 1

Examination of the thyroid gland revealed a firm mass with vague lobulation, which on sectioning showed a diffuse infiltrate of large centroblast-like cells and residual thyroid follicles (Figure 1A). Scattered mitotic figures and apoptotic cells, as well as foci of coagulative necrosis, were seen. No low-grade lymphoma component or lymphoepithelial lesions were identified. Immunohistochemistry and flow cytometry findings confirmed the diagnosis of primary thyroid DLBCL, non-germinal centre B-cell (non-GCB) phenotype (Figure 1B–1D, Table 1). Approximately, 60% of the neoplastic cells showed aberrant nuclear p53 staining, and the lymphoma had a high Ki-67 proliferation index (90%). A clonal product was identified on PCR analysis for *IGH* gene rearrangement.

G-band analysis demonstrated a complex karyotype (Figure 1E, Table 1). FISH analysis detected *KMT2A* translocation in 94% cells (Figure 1F and 1G) and *IGH* translocation in 95% cells using break-apart probes. The signal patterns of the *IGH* and *KMT2A* probes on metaphase spreads confirmed the karyotypic observation of t(11;14)(q23;q22). However, the breakpoint involving *KMT2A* was unusual, as the 3′ (distal, orange) *KMT2A* signal that translocated to der(14) also had a tiny signal from the 5′(proximal, green) *KMT2A* probe. Thus, the breakpoint in the *KMT2A* gene was proximal to the conventional breakpoint that completely separates the 5′ (green) signal from the 3′ (orange) signal. In addition, an extra copy of the 3′ (orange) *KMT2A* probe was also seen on a small acrocentric chromosome (Figure 1G). These results suggest that the *KMT2A* gene was involved in complex rearrangements with *IGH* and another unidentifiable gene/locus. No

DOI: 10.1002/hon

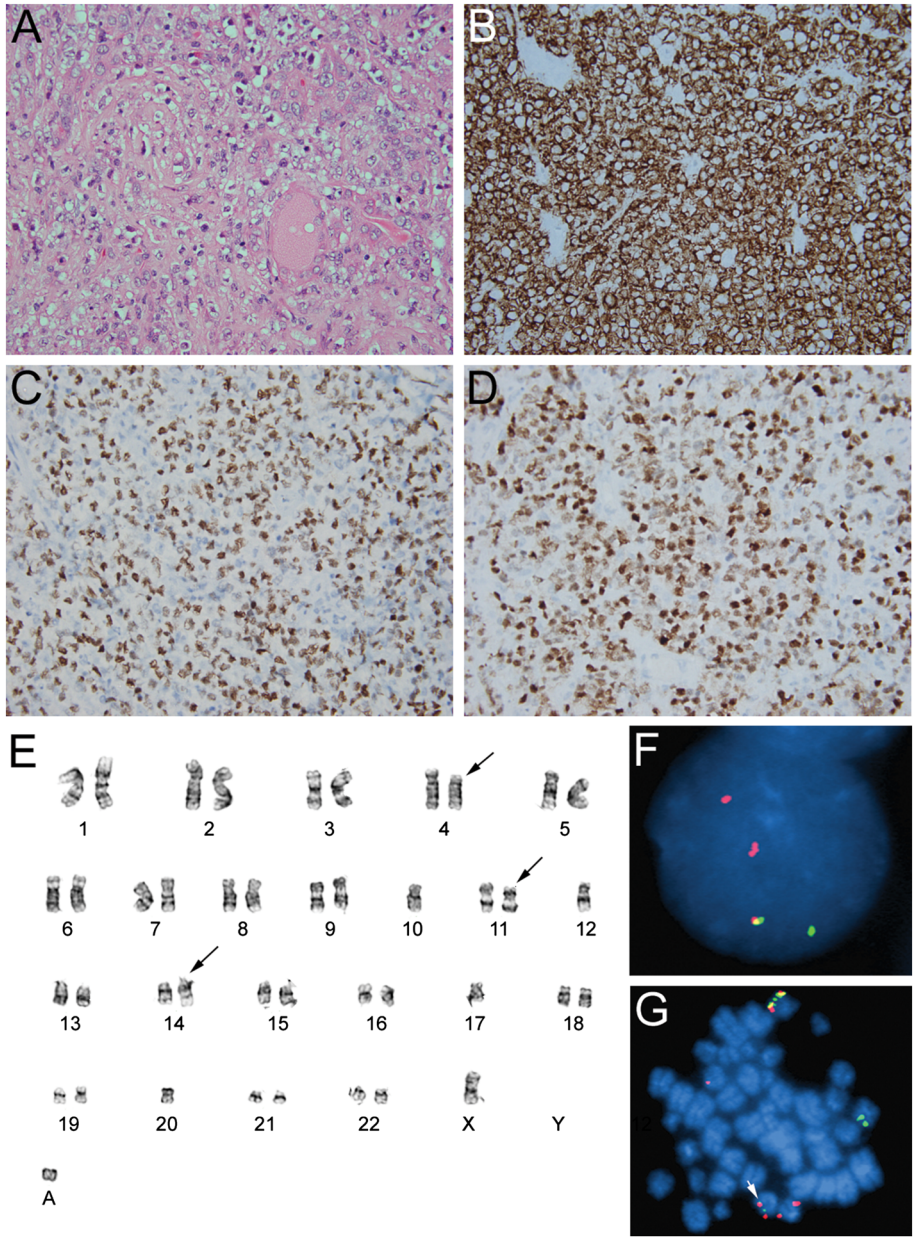

Figure 1. (A) Large centroblast-like cells infiltrating the thyroid gland (hematoxylin and eosin, 400×) display CD20 (B), MUM1 (C) and BCL6 (D) expression, consistent with DLBCL, non-GCB phenotype. E, G-band karyotype, arrows indicate t(11;14)(q23;q32) and del (4)(p12). Fluorescence *in situ* hybridization analysis using *KMT2A* break-apart probes in interphase nuclei (F) and a metaphase spread (G) shows one yellow signal (normal, non-rearranged *KMT2A*), one green signal (5′ rearranged), one orange and faint green signal (3′ atypical 5′ proximal break point) (white arrow) and one additional orange signal (3′ rearranged *KMT2A* present on a small acrocentric chromosome), findings consistent with a complex *KMT2A* translocation

BCL2 or *BCL6* rearrangements were detected. FISH analysis using *ATM*/*TP53* probes revealed deletion of one copy of *TP53* in 95% of cells, consistent with the karyotypic identification of loss of chromosome 17.

Case 2

The spleen had a diffuse, micronodular appearance on gross examination, and two discrete large parenchymal nodules as well as a hilar mass were visualized. Sections of the hilar lymph node and parenchymal nodules showed diffuse infiltrates of large lymphocytes with immunoblastic and focal plasmacytoid features (Figure 2A). The splenic infiltrates were surrounded by fibrous bands and abundant hemosiderin-laden macrophages were present. Scattered apoptotic debris, mitoses and foci of coagulative necrosis were observed. Immunohistochemistry and flow cytometry confirmed the presence of a DLBCL exhibiting a non-GCB phenotype (Figure 2C–2F, Table 1). The proliferation index was elevated (Ki-67, 80%), and approximately 80% of the

DOI: 10.1002/hon

Table 1. B-cell non-Hodgkin lymphomas with *KMT2A* gene translocations

Case	Age/sex	G-band karyotype	FISH	Phenotype	Diagnosis	Therapy	Outcome	Ref.
1	70/M	44,X,-Y,del(4)(p12),t(11;14)(q23;q32),−17,r(20)(p13q13.3)[13]/44,idem,t(1;9)(p36.1;q34)[4]/45,idem,+21[3]	*KMT2A* -T	CD20+, CD10(weak)+, CD5-, CD43-, BCL6+, MUM1+, and BCL2+, Kappa light chain restricted[a], p53 60%, Ki67 90%	Primary thyroid DLBCL	R-CHOP 6 cycles	7 years clinical remission	Current case
2	68/F	48,XX,+3,t(3;11)(p23;q23),add(17)(p12),+18[6]/46,idem,add(6)(p21),−16,18[6]/49,idem, +9, ider(15)(q10)del(15)(q11.2q14)[16]	*KMT2A*-T	CD20+, CD79a+, CD10−, BCL6+, MUM1+, BCL2+, CD5−,and CD43(weak, focal)+, Kappa light chain restricted, p53 80%, Ki67 80%.	DLBCL arising from SMZL	R-CHOP 6 cycles	2.5 years clinical remission	Current case
3	NR	t(14;18)(q32;q21) and t(6;11)(p12;q23)	NP[b]	NR	FL	NR	NR	[11]
4	NR	t(11;18)(q23;q21) and other aberrations	NP[b]	NR	DLBCL	NR	NR	[11]
5	NR	t(8;14)(q24;q32) and inv(11)(q14q23)	NP[b]	NR	Burkitt lymphoma	NR	NR	[11]
6	2/M	t(4;11)(q21;q23)	*KMT2A* -T	CD19+, CD20+, CD22+, sIgM+, sIgD+, TdT−, CD3−, MPO−[a]	PTLD Burkitt-like lymphoma	Combination chemotherapy	15 mo. clinical remission	[8]

FISH, fluorescence *in situ* hybridization using *KMT2A* break-apart probes; *KMT2A*-T, *KMT2A* gene translocation; PTLD, post-transplant lymphoproliferative disorder; FL, follicular lymphoma; R-CHOP, cyclophosphamide, hydroxydaunomycin, vincristine, prednisone and rituximab; combination chemotherapy, prednisone, vincristine, doxorubicin, cyclophosphamide and methotrexate; NR, not recorded; NP, not performed.

[a]Using flow cytometry.

[b]*KMT2A* rearrangements were identified by Southern blot analysis.

DOI: 10.1002/hon

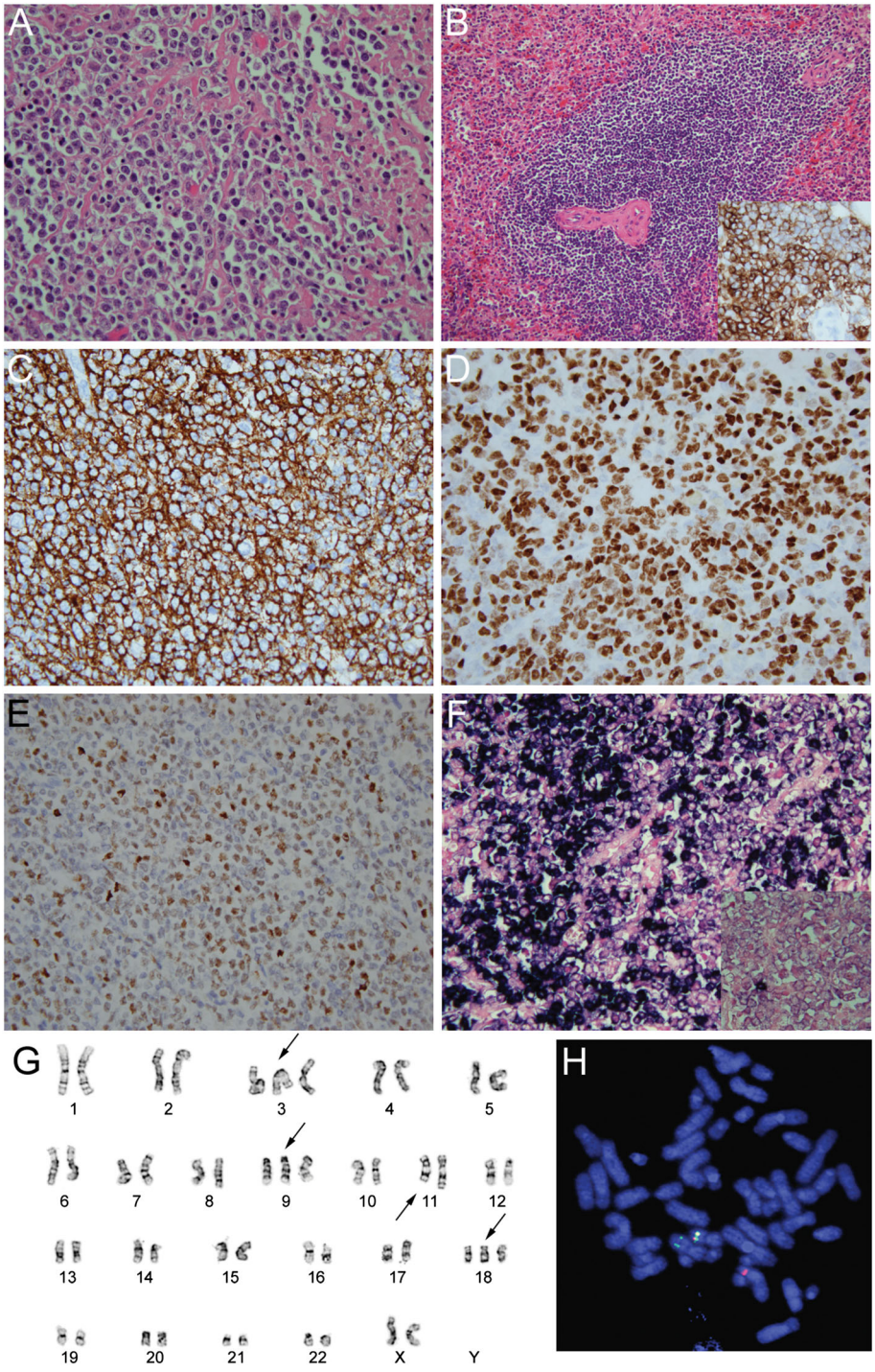

Figure 2. Splenic mass displaying diffuse large B-cell lymphoma (DLBCL) (A) and adjacent spleen exhibiting splenic marginal zone lymphoma (B) (insert shows dim CD43 expression on neoplastic cells) (hematoxylin and eosin, 400×). DLBCL expresses CD20 (C), MUM1 (D) and BCL6 (E), consistent with a non-GCB phenotype. (F) Neoplastic cells show kappa light chain restriction by *in situ* hybridization for immunoglobulin light chain mRNA (insert shows rare cells expressing lambda light chain mRNA). G, G-band karyotype obtained from splenic DLBCL. Arrows indicate t(3;11)(p23;q23),+3, +9 and +18. (H) Fluorescence *in situ* hybridization analysis using *KMT2A* break-apart probe on a metaphase spread shows one yellow signal (intact *KMT2A* locus) on normal chromosome 11, one green signal (rearranged, 5′ end) on the short arm of abnormal chromosome 3 and one orange signal (rearranged 3′ end) on the long arm of abnormal chromosome 11, features consistent with *KMT2A* translocation

neoplastic cells showed aberrant nuclear p53 staining. Elsewhere, the splenic parenchyma showed variably sized white pulp lymphoid nodules that mostly lacked germinal centres and were comprised of small lymphocytes (Figure 2B) that displayed variable plasmacytoid features and had the following phenotype: CD20+, CD79a+, BCL6-,

DOI: 10.1002/hon

CD10-, MUM1(subset)+, CD5-, and CD43(subset)+ (Figure 2B (insert)). Staining for Ki-67 showed a low proliferation index (10%). These features were suggestive of SMZL.

G-band analysis of the large cell lymphoma demonstrated a complex karyotype (Figure 2G, Table 1). FISH analysis using the *KMT2A* break-apart probe detected *KMT2A* translocation in 66.4% cells (Figure 2H). FISH analyses using *IGH*, *BCL2* or *BCL6* break-apart probes were negative for translocations. However, three copies of *BCL2* were observed in 38% cells, with multiple copies (up to 10/cell) noted in a subclone comprising 46% cells. The BCL6 probe showed three copies in 82% cells. These findings confirmed the presence of trisomy 3 and 18 seen on karyotype analysis. FISH using *ATM*/*TP53* probes revealed deletion of one copy of *TP53* in 77% of cells. A sample corresponding to the SMZL showed a normal karyotype and no *KMT2A* gene translocation. However, trisomy 18 was detected in 7% of cells using the *BCL2* probe.

Clonal products of identical molecular weight were detected by PCR analysis for *IGH* gene rearrangement in the SMZL and DLBCL components. On the basis of the morphologic, phenotypic, cytogenetic and molecular analyses, the findings were indicative of large cell transformation of SMZL.

Discussion

We describe two cases of DLBCL harbouring *KMT2A* translocations. A review of the literature disclosed only four prior reports of B-NHL associated with *KMT2A* translocations (Table 1). In the largest series of NHL with karyotype abnormalities involving the 11q23 region, three of 20 (15%) cases harboured *KMT2A* translocations, including one case each of follicular lymphoma, Burkitt lymphoma and DLBCL [11]. No morphologic and phenotypic details were reported for these cases, and no information regarding treatment and outcomes was provided. An EBV-associated post-transplant Burkitt-like lymphoma with *KMT2A* translocation was also described in a 28-month male patient who presented with abdominal lymphadenopathy and involvement of the liver and kidney, 19 months after liver transplantation [8]. Only limited phenotypic information was provided, but the patient was in complete remission 15 months after withdrawal of immunosuppression and administration of combination chemotherapy (Table 1).

Neither primary thyroid DLBCL, nor large cell transformation of SMZL with abnormalities involving *KMT2A* have been reported previously. DLBCL and marginal zone lymphomas, comprise up to 90% of all primary thyroid lymphomas, and an association between DLBCL and thyroid marginal zone lymphoma and chronic lymphocytic thyroiditis is well recognized [14,15]. Molecular pathways of thyroid lymphoma development are thought to differ from lymphomas occurring at other sites, but the molecular or genetic alterations underlying primary, de novo DLBCL of the thyroid are not well understood. According to the Mitelman Database of Chromosome Aberrations and Gene Fusions in Cancer [16] cytogenetic aberrations of only six cases of primary thyroid DLBCL have been reported. The cases harbouring structural changes included two with t(8;14)(q24;q32) involving the *cMYC* and *IGH* genes and one displaying t(12;14)(p11.2;q32.3). Numerical chromosomal abnormalities included loss of the X chromosome and trisomy 22. Data regarding genetic or molecular alterations associated with large cell transformation of SMZL are even sparser. In a series of 12 SMZL transforming to DLBCL, cytogenetic findings were described for seven cases [17]. Six of seven cases showed chromosome abnormalities, with recurrent 7q losses observed in 42% and 1q32 alterations in 29% of cases. The lack of molecular alterations of *TP53* and infrequent loss of the p16 protein in the subset of cases analyzed, led the investigators to speculate that the pathways of SMZL transformation might be different from those described for other low-grade B-NHL [17].

KMT2A is a member of the *lysine N-methyltransferase* family of genes that encode SET domain containing proteins, which provide an epigenetic mark at gene regulatory regions, especially enhancers, by modifying (methylating) lysine-4 of histone 3. This change is required for the activation of a large number of target genes involved in hematopoiesis and development, most notably the homeobox (*HOX*) gene family [18]. *KMT2A* plays important roles in a variety of cellular functions, including DNA damage response and cell cycle control, by regulating cell cycle checkpoints and preventing chromatid errors [19,20]. A multitude of *KMT2A* aberrations have been documented in hematologic neoplasms, including translocations, partial tandem duplications, amplifications and mutations, which arise via diverse mechanisms and have different functional consequences [6,21]. *KMT2A* translocations or rearrangements represent the most common abnormalities that result in the formation of chimeric transcripts with leukemogenic potential [22]. To date, at least 121 different *KMT2A* translocations and 79 *KMT2A* fusion partner genes have been identified in acute leukemias and myeloid neoplasms [23]. The resulting chimeric proteins differentially impact the phenotype and outcome of the neoplasms by interacting with various molecular complexes, regulating different networks of genes, and/or having differential effects on common targets [20]. *HOXA9* and its transcriptional co-factor *MEIS1* are the most critical downstream targets deregulated by *KMT2A* fusion proteins, as their co-expression is sufficient to transform cells and induce acute myeloid leukemia [24]. Additionally, *KMT2A*-fusion proteins exhibit resistance to degradation by the ubiquitin-proteasome system, which may contribute to their leukemogenic potential [19].

The functional consequences of *KMT2A* translocations in mature B-NHL, including the two DLBCL presented

DOI: 10.1002/hon

herein are not known at present. Deregulated expression of *KMT2A* via juxtaposition with the immunoglobulin heavy chain, or another, enhancer could result in a gain of function. However, other possibilities include, loss of function due to structural changes, such as deletions within *KMT2A*, via a dominant negative effect by interfering with wild-type *KMT2A*, or altered function due to the generation of fusion transcripts. Further *in vitro* studies, modelling B-NHL associated *KMT2A* translocations, are required to determine if these rearrangements alter associations between *KMT2A* and other cofactors or signalling complexes, as has been observed in acute leukemias harbouring *KMT2A* translocations and also for products of other genes targeted by recurrent translocations in subsets of NHL.

In contrast to translocations, amplifications of the 11q23 region including the *KMT2A* locus have been documented more frequently in B-NHL. Starostik *et al*. demonstrated high level amplifications of *KMT2A* in five cases of primary gastric DLBCL using comparative genomic hybridization and FISH analyses [25]. Two additional reports described *KMT2A* amplifications in one case each of a plasmablastic lymphoma [10] and an intravascular large B-cell lymphoma [9]. The former exhibited five copies of *KMT2A* by cytogenetic analysis, occurred in an HIV+ patient and responded to standard chemotherapy [10]. Of note, amplifications of the chromosome 11q23 region have been described in intravascular large B-cell lymphomas; however, *KMT2A* amplification has been confirmed in only one case by FISH analysis [9]. If the amplifications are established to involve wild-type *KMT2A*, then such abnormalities could result in *KMT2A* gain of function and have similar pathogenetic consequences as suggested for myeloid neoplasms associated with *KMT2A* amplifications, but different from those proposed for neoplasms harbouring partial tandem duplications [21].

Further molecular studies analysing the chromosome breakpoints are required to determine the plausible mechanisms responsible for generating *KMT2A* translocations in mature B-NHL. Acute leukemia and MDS associated *KMT2A* translocations arise due to inhibition of the enzyme DNA topoisomerase II by chemotherapeutic drugs [26]. Our patients had no history of exposure to topoisomerase II inhibitors, as well as alkylating agents or radiation, which have also been implicated in the genesis of *KMT2A* translocations. The mechanistic basis of other types of *KMT2A* aberrations in leukemias, MDS and B-NHL is not well understood. *KMT2A* abnormalities have been associated with a poor prognosis in MDS and acute leukemias [6]. On the contrary, both our DLBCL as well as previously reported B-NHL subtypes associated with *KMT2A* translocations or amplifications responded well to standard chemotherapy regimens and showed complete remission, albeit with variable follow-up durations, ranging from 15 months to 7 years (Table 1).

Recent studies using high resolution genomic approaches have uncovered aberrations (mostly mutations) in several epigenetic modifier genes, especially those regulating histone acetylation and methylation in lymphomas, as well as other malignancies [4,5,27,28]. Of note, these studies identified mutations in multiple other *lysine N-methyltransferase* gene family members. Loss of function mutations in *KMT2D/MLL2* were the most frequent reported events in DLBCL (up to 32% of cases), but their role in DLBCL pathogenesis is not known at present [4,5].

In summary, our and the few previously reported cases document the occurrence of *KMT2A* translocations in mature B-NHL, besides acute leukemias and MDS, and suggest that *KMT2A* aberrations represent, as yet, underappreciated (and additional) mechanisms deregulating the function of epigenetic modifier genes in DLBCL. Future investigations of B-NHL associated with chromosome 11q23 aberrations are warranted to shed light on the frequency of *KMT2A* abnormalities in different disease subtypes, better understand the stage of acquisition of these alterations and elucidate their functional consequences.

Conflict of interest

The authors have no competing interest.

References

1. Schneider C, Pasqualucci L, Dalla-Favera R. Molecular pathogenesis of diffuse large B-cell lymphoma. *Semin Diagn Pathol*. 2011; **28**(2): 167–177.
2. Tagawa H, Suguro M, Tsuzuki S, et al. Comparison of genome profiles for identification of distinct subgroups of diffuse large B-cell lymphoma. *Blood* 2005; **106**(5): 1770–1777.
3. Swerdlow SH CE, Harris NL, Jaffe ES, Pileri SA, Thiele J, Vardiman JW. WHO classification of tumours of haematopoietic and lymphoid tissues. 4 ed. Lyon International Agency for Research on Cancer; 2008.
4. Pasqualucci L, Trifonov V, Fabbri G, et al. Analysis of the coding genome of diffuse large B-cell lymphoma. *Nature genetics* 2011; **43**(9): 830–837.
5. Morin RD, Mendez-Lago M, Mungall AJ, et al. Frequent mutation of histone-modifying genes in non-Hodgkin lymphoma. *Nature*. 2011; **476**(7360): 298–303.
6. Muntean AG, Hess JL. The pathogenesis of mixed-lineage leukemia. *Annual review of pathology* 2012; **7**: 283–301.
7. Tanaka K, Eguchi M, Eguchi-Ishimae M, et al. Restricted chromosome breakpoint sites on 11q22-q23.1 and 11q25 in various hematological malignancies without MLL/ALL-1 gene rearrangement. *Cancer genetics and cytogenetics* 2001; **124**(1): 27–35.
8. Corapcioglu F, Olgun N, Sarialioglu F, Uysal KM, Oren H, Sercan O. MLL-AF4 gene rearrangement in a child with Epstein-Barr virus-related posttransplant B-cell lymphoma. *Journal of pediatric hematology/oncology*. 2003; **25**(9): 740–742.
9. Deisch J, Fuda FB, Chen W, et al. Segmental tandem triplication of the MLL gene in an intravascular large B-cell lymphoma with multisystem involvement: a comprehensive morphologic, immunophenotypic, cytogenetic, and molecular cytogenetic antemortem study. *Archives of pathology & laboratory medicine*. 2009; **133**(9): 1477–1482.

10. Reddy KS, Parsons L, Mak L, Chan JA. An HSR on chromosome 7 was shown to be an insertion of four copies of the 11q23 MLL gene region in an HIV-related lymphoma. *Cancer genetics and cytogenetics*. 2001; **129**(2): 107–111.
11. Thirman MJ, Gill HJ, Burnett RC, et al. Rearrangement of the MLL gene in acute lymphoblastic and acute myeloid leukemias with 11q23 chromosomal translocations. *The New England journal of medicine* 1993; **329**(13): 909–914.
12. International Standing Committee on Human Cytogenetic Nomenclature, Shaffer LG, Slovak ML, Campbell LJ. ISCN 2009: An International System for Human Cytogenetic Nomenclature. Karger: Basel; Unionville, CT, 2009.
13. Langerak AW, Molina TJ, Lavender FL, et al. Polymerase chain reaction-based clonality testing in tissue samples with reactive lymphoproliferations: usefulness and pitfalls. A report of the BIOMED-2 concerted action BMH4-CT98-3936. *Leukemia* 2007; **21**(2): 222–229.
14. Graff-Baker A, Sosa JA, Roman SA. Primary thyroid lymphoma: a review of recent developments in diagnosis and histology-driven treatment. *Curr Opin Oncol* 2010; **22**(1): 17–22.
15. Taniwaki M, Nishida K, Misawa S, et al. Correlation of chromosome abnormalities with clinical characteristics in thyroid lymphoma. *Cancer* 1989; **63**(5): 873–876.
16. Mitelman database of chromosome aberrations and gene fusions in cancer [Internet]. 2012. Available from: http://cgap.nci.nih.gov/Chromosomes/Mitelman.
17. Camacho FI, Mollejo M, Mateo MS, et al. Progression to large B-cell lymphoma in splenic marginal zone lymphoma: a description of a series of 12 cases. *Am J Surg Pathol* 2001; **25**(10): 1268–1276.
18. Yu BD, Hess JL, Horning SE, Brown GA, Korsmeyer SJ. Altered Hox expression and segmental identity in MLL-mutant mice. *Nature* 1995; **378**(6556): 505–508.
19. Liu H, Cheng EH, Hsieh JJ. Bimodal degradation of MLL by SCFSkp2 and APCCdc20 assures cell cycle execution: a critical regulatory circuit lost in leukemogenic MLL fusions. *Genes & development* 2007; **21**(19): 2385–2398.
20. Ballabio E, Milne TA. Molecular and Epigenetic Mechanisms of MLL in Human Leukemogenesis. *Cancers* 2012; **4**(3): 904–944.
21. Basecke J, Whelan JT, Griesinger F, Bertrand FE. The MLL partial tandem duplication in acute myeloid leukaemia. *British journal of haematology* 2006; **135**(4): 438–449.
22. Marschalek R. Mechanisms of leukemogenesis by MLL fusion proteins. *British journal of haematology* 2011; **152**(2): 141–54.
23. Meyer C, Hofmann J, Burmeister T, et al. The MLL recombinome of acute leukemias in 2013. *Leukemia* 2013; **27**(11): 2165–2176.
24. Li Z, Huang H, Chen P, *et al.* miR-196b directly targets both HOXA9/MEIS1 oncogenes and FAS tumour suppressor in MLL-rearranged leukaemia. *Nature communications* 2012; **3**: 688.
25. Starostik P, Greiner A, Schultz A, et al. Genetic aberrations common in gastric high-grade large B-cell lymphoma. *Blood* 2000; **95**(4): 1180–1187.
26. Mosad E, Abdou M, Zaky AH. Rearrangement of the myeloid/lymphoid leukemia gene in therapy-related myelodysplastic syndrome in patients previously treated with agents targeting DNA topoisomerase II. *Oncology* 2012; **83**(3): 128–134.
27. Lawrence MS SP, Mermel CH, Robinson JT, et al. Discovery and saturation analysis of cancer genes across 21 tumour types. *Nature* 2014; 23;**505**(7484): 495–501.
28. Herz HM, Hu D, Shilatifard A. Enhancer malfunction in cancer. *Molecular cell* 2014; **53**(6): 859–866.

DOI: 10.1002/hon